REPORTS

MICROPOROUS NETWORKS

A metal-organic framework–based splitter for separating propylene from propane

A. Cadiau,[1]* K. Adil,[1]* P. M. Bhatt,[1] Y. Belmabkhout,[1] M. Eddaoudi[1,2]†

The chemical industry is dependent on the olefin/paraffin separation, which is mainly accomplished by using energy-intensive processes. We report the use of reticular chemistry for the fabrication of a chemically stable fluorinated metal-organic framework (MOF) material (NbOFFIVE-1-Ni, also referred to as KAUST-7). The bridging of Ni(II)-pyrazine square-grid layers with $(NbOF_5)^{2-}$ pillars afforded the construction of a three-dimensional MOF, enclosing a periodic array of fluoride anions in contracted square-shaped channels. The judiciously selected bulkier $(NbOF_5)^{2-}$ caused the looked-for hindrance of the previously free-rotating pyrazine moieties, delimiting the pore system and dictating the pore aperture size and its maximum opening. The restricted MOF window resulted in the selective molecular exclusion of propane from propylene at atmospheric pressure, as evidenced through multiple cyclic mixed-gas adsorption and calorimetric studies.

Olefin/paraffin separation is a critical separation for the chemical industry. It is mainly accomplished by means of cryogenic distillation, which accounts for nearly 3% [120 tera–British thermal units (TBtu)/year] of the total energy used for separations (1). Exploratory olefin/paraffin separation studies that used conventional adsorbents such as zeolites and ultramicroporous carbon revealed the lack of a suitable adsorbent with the appropriate pore system (functionality and/or aperture size) that could selectively discriminate and separate the two relevant vapors with a noticeably reduced energy footprint (2).

Propylene is a prime olefin raw material for petrochemical production, second in importance to ethylene, and is an essential building block for the manufacturing of various chemicals, including polypropylene (3). Propylene purity guides its end use because polypropylene requires a high-purity propylene with 99.5 weight % (wt %) minimum (polymer-grade specifications), whereas chemical-grade specifications typically involve a propylene purity of 92% or more. The purity of propylene primarily depends on the removal of propane; this separation process is energy-intensive and conventionally dominated by the cryogenic

distillation because of the close-boiling points and the slight variance in the condensabilities of the two components. Researchers have been exploring various separation methods, including (i) the π complexation–driven separation (as adsorbent or facilitated membrane) (4, 5) or (ii) separation based on kinetics by using physical adsorbents (zeolites A) or membranes, driven mainly by the difference in diffusion rates into the pore system (6, 7). Thus far, adsorbents and membranes reported for this task used a partial size-shape sieving–based separation process and displayed low to moderate separation factors, as exemplified in the case of zeolites (8, 9) and carbon molecular sieves (7) encompassing contracted pore sizes. The full extraction of propylene from propane by using adsorbent-based separating agents has yet to be demonstrated and accomplished. This is due to (i) the close structural dimensions of propylene and propane molecules, in addition to their associated similar physical properties, and (ii) difficulties in fine-tuning the pore aperture size in 0.2 to 1 Å scale increments in a given ultramicropore adsorbent material with a suitable pore system size ranging between 3 and 5 to 6 Å.

Ideally, porous materials constructed by means of the molecular building block approach offer potential to attain the requisite separation through selective molecular exclusion, in which the molecular building blocks could be adopted in shape, size, and functionality so as to produce a suitable pore aperture size that can selectively separate molecules with almost identical physical properties. We recently succeeded in selectively separating branched paraffins from normal paraffins by

fine-tuning a metal-organic framework (MOF) aperture size to completely exclude branched paraffins (10).

MOF materials represent a tunable class of hybrid solid-state materials that consist of metal nodes or metal clusters coordinated to multifunctional organic linkers (11–13). MOFs have received considerable attention as adsorbents for gas storage applications (14–17) and have demonstrated high potential for equilibrium- and/or kinetic-based gas separations, such as CO_2/N_2 or CO_2/H_2 (18–22). MOF chemistry has permitted the prospective fabrication of porous materials with a high degree of structural predictability and subsequently a precise control of window apertures size and shape at the molecular level, in contrast to those of zeolites, carbon, and polymeric-based materials (10).

We demonstrate a full molecular exclusion of propane from propylene at standard ambient temperature and pressure using a fluorinated porous MOF adsorbent, KAUST-7. The reticular chemistry (23) approach was used to construct this material based on pillared square-grids strategy—two-dimensional nets based on linked metal nodes that are pillared via a specific inorganic molecular building block in the third dimension so as to form a three-periodic net with a primitive cubic topology (Fig. 1).

Previously, we applied coordination chemistry principles to demonstrate that the introduction of specific cations—Zn^{2+}, Ni^{2+}, and Cu^{2+}—into the metal-pyrazine square-grid layers has an impact on the unit cell volume and more precisely on the pore size, which resulted in an enhancement of the CO_2-framework energy interaction. This family of materials possesses distinct CO_2 capture properties, especially at very low concentrations, which is ideal for postcombustion capture and air-capture application (24). Nevertheless, the SIFSIX-3-Ni (Fig. 1, C and E) was found to adsorb both propylene and propane.

Substitution of the metal node in the SIFSIX (24) platform permitted the fine-tuning of the aperture size and pore contraction and subsequent CO_2 capture properties. In order to explore the possibility of further tuning this platform, we closely examined the structural features of the SIFSIX platform (Figs. 1 and 2) (24) and identified an alternative pathway to potentially further fine-tune the pore aperture size. The hindered free rotation of the pyrazine-bridging ligands, by altering the nature, shape, and dimensions of the pillars used, dictates the pore aperture size and its maximum opening. This approach offers the potential to select for the passing or blocking of specific probe molecules.

To construct the targeted material with these envisioned structural features, we opted to maintain the Ni(II) as a six-connected node, connecting the pyrazine ligands in square grid–like layers, and to modify the inorganic pillars. We anticipated that using a pillar with a bigger cation (Nb^{5+} instead of Si^{4+}) would result in a relatively shorter proximal distance between the adjacent fluorine centers and consequently contract the aperture size of the channels (Fig. 2). Reactions between

Ni(NO$_3$)$_2$•6H$_2$O, Nb$_2$O$_5$, HF$_{aq}$, and pyrazine (pyr) in water yielded purple square-shaped crystals. The single-crystal x-ray diffraction data revealed the anticipated primitive-cubic structure, formulated as NiNbOF$_5$(pyr)$_2$•2H$_2$O, in good agreement with the elemental analysis and the thermal gravimetric analysis (TGA) results (supplementary materials, materials and methods, and fig. S6). The phase purity of resultant fluorinated MOF material, referred to as NbOFFIVE-1-Ni or KAUST-7, was confirmed by using a full pattern matching by means of the Le Bail method (fig. S1).

The assignment of fluorine atoms in equatorial positions within the pillar has been previously demonstrated in similar materials (25, 26). The particular use of (NbOF$_5$)$^{2-}$ as the pillaring inorganic building block, instead of (SiF$_6$)$^{2-}$, resulted in a longer metal-fluorine distance (1.95 Å) and a subsequent tilting of pyrazine molecules (Figs. 1 and 2) (19, 24). Analysis of the NbOFFIVE-1-Ni structure (collected at 100 K) revealed the plausible smallest pore window opening associated with the relatively hindered rotation of the (NbOF$_5$)$^{2-}$ pillars, reinforced by the presence of hydrogen bond interactions (Fig. 2 and fig. S3). As a result, the hydrogen atoms of the pyrazine linkers circumference the resultant square-shaped channels with a reduced pore aperture size of 3.0471(1) Å [versus 5.032(1) Å for SIFSIX-3-Ni] (Fig. 1B), prohibiting the diffusion of any molecule other than water (numbers in parentheses indicate the 1 SD uncertainty in the final digits). In order to gain a better insight on the plausible rotation and tilting of the pyrazine linker, and subsequently derive a relative maximum opening of the window, providing a gate limit for the largest molecule to pass through, we collected and analyzed the same structure at room temperature. No structural differences were detected from single-crystal x-ray data collected at room temperature and the cryogenic temperature. The thermal ellipsoids analysis revealed a certain degree of rotation of (NbOF$_5$)$^{2-}$ pillars, whereas the pyrazine molecules were crytallographically well localized. The (NbOF$_5$)$^{2-}$ pillars and pyrazine molecules were interconnected through a network of strong hydrogen bonding interactions [F–H 2.483(1) Å]. The noticeably small pore aperture size, derived from the crystal structure at room temperature, suggests that the passing of the propylene molecules is governed by the plausible gate opening associated with the extra tilting of the pyrazine molecules under propylene gas stimuli. The pore aperture size is regulated by the presence or omission of the steric hindrance between pyrazine molecules and (NbOF$_5$)$^{2-}$ pillars, and the lack of a precise kinetic diameter for propylene in the open literature makes precise quantification difficult. Presumably, the plausible complete omission of the occurring steric hindrance can afford a theoretical maximum pore aperture size of 4.752(1) Å (Fig. 1D).

To further confirm the restricted pore size opening owing to the hindered rotation of pyrazine ligands at low temperature, we performed adsorption studies on the fully evacuated NbOFFIVE-1-Ni. As anticipated, NbOFFIVE-1-Ni did not adsorb N$_2$ at 77 K, indicating the restricted access to N$_2$ at this low cryogenic temperature due to the contracted pore aperture size. On the other hand, adsorption studies performed at room temperature by using CO$_2$ as the adsorbate molecule revealed that NbOFFIVE-1-Ni is microporous,
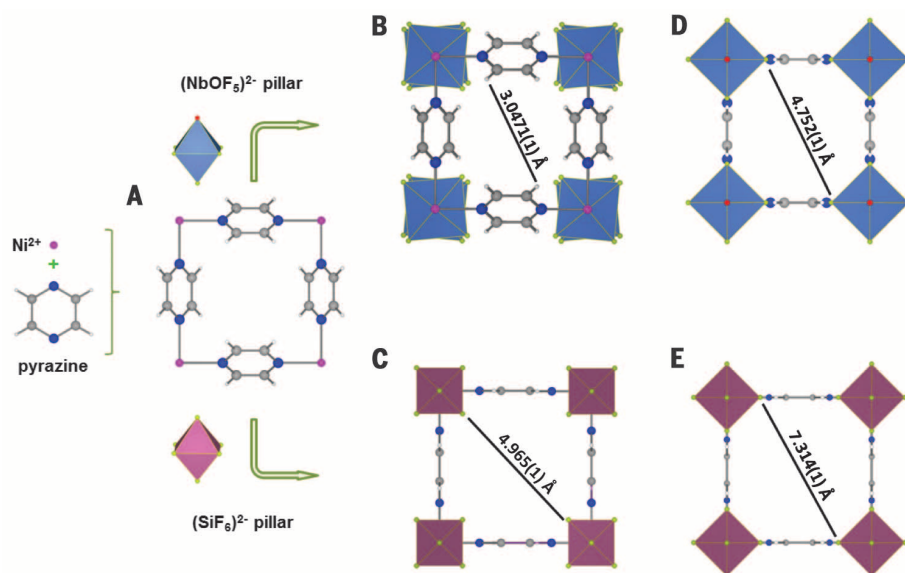

Fig. 1. Structure description of NbOFFIVE-1-Ni highlighting the building blocks arrangement and its comparison with the parent SIFSIX-3-Ni. (**A**) Illustration of the square-shaped arrangement in the Ni-pyrazine (4,4') square grid that is further pillared by inorganic blocks [(NbOF$_5$)$^{2-}$ or (SiF$_6$)$^{2-}$] to generate a three-dimensional MOF with a primitive cubic topology. (**B**) Crystal structure of NbOFFIVE-1-Ni at 100 K, showing the titling of pyrazine molecules. (**C**) Crystal structure of SIFSIX-3-Ni at 298 K. (**D**) Simulation of the maximum open structure of NbOFFIVE-1-Ni, showing a theoretical window size of 4.752(1) Å. (**E**) Simulation of the maximum open structure of SIFSIX-3-Ni, showing a theoretical window size of 7.314(1) Å.

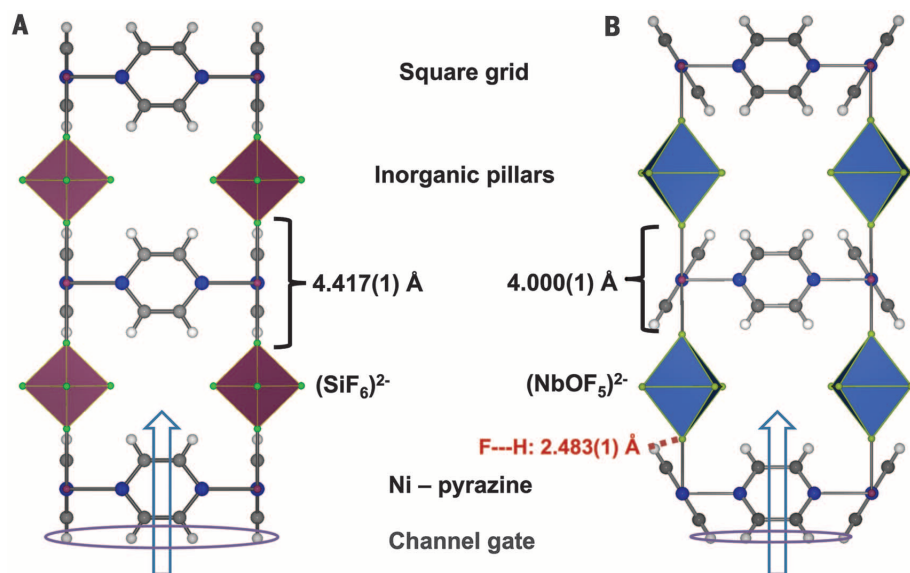**Fig. 2. Structure comparison between SIFSIX-3-Ni and NbOFFIVE-1-Ni showing the impact of the use of a relatively bigger inorganic pillar [(NbOF$_5$)$^{2-}$ instead of (SiF$_6$)$^{2-}$].** (**A**) [010]-projection view of SIFSIX-3-Ni, showing the perfectly aligned pyrazine molecules. (**B**) [010]-projection view of NbOFFIVE-1-Ni, showing the titling of pyrazine molecules due to the use of the bigger (NbOF$_5$)$^{2-}$ building block. The shorter distance between two (NbOF$_5$)$^{2-}$ building blocks from the two neighboring layers [4.000(1) Å versus 4.417(1) Å in the case of (SiF$_6$)$^{2-}$ pillars in the SIFSIX-3-Ni] induces a titling of pyrazine molecules and consequently a decrease in the pore aperture size, comparatively with that of SIFSIX-3-Ni.

with an apparent surface area of 280 m²/g and an estimated pore volume of 0.095 cm³/g (fig. S8).

The permanent porosity and the associated restricted pore aperture size [maximum 4.752(1) Å] prompted us to assess and evaluate the adsorption properties of NbOFFIVE-1-Ni for various key probe molecules characterized by different shapes and a comparatively larger kinetic diameter. Specifically, adsorption properties of molecules that are relevant to both industrial gases upgrading and the challenging olefin/paraffin separation—namely methane (CH_4), ethane (C_2H_6), ethylene (C_2H_4), propylene (C_3H_6), and propane (C_3H_8)—were evaluated at room temperature and atmospheric pressures.

Before assessing the NbOFFIVE-1-Ni as a potential separating agent, we evaluated its stability against water vapor and H_2S by monitoring the powder x-ray diffraction (PXRD) patterns upon exposure to various humidity levels and H_2S concentrations (Fig. 3A and fig. S4). Evidently, no loss of crystallinity and no phase change were observed during the exposure of the material to humidity from 5 to 95% (fig. S4), H_2O (fig. S7), or H_2S (up to 10%) (fig. S9). The hydrolytic sta-

bility of KAUST-7 is supported by the retention of the material CO_2 adsorption uptake and structural integrity after its immersion in aqueous solution for more than 6 months. The performance of the material was not altered as the maximum CO_2 uptake was reached (fig. S10). Moreover, the NbOFFIVE-1-Ni is proven to be highly thermal stable, as evidenced through thermogravimetric analysis (TGA) and variable temperature PXRD patterns (fig. S5 and S6).

Single-gas adsorption data revealed that the NbOFFIVE-1-Ni channels with restricted aperture size allowed the adsorption of C_3H_6 but did not permit the C_3H_8 to diffuse/adsorb into the pore system at 298 K up to ~1 bar (Fig. 3B). Considerably, C_3H_6/C_3H_8 50/50 mixed-gas adsorption data, collected at 298 K (up to 0.5 bar partial pressure of C_3H_6), overlaid with the pure C_3H_6 adsorption isotherm (Fig. 3B), which supports the molecular exclusion of propane from propylene. The concomitant pore aperture size and shape expressed in this MOF adsorbent provide the requisite size and shape cut-off in adsorption, resulting in the observed C_3H_6/C_3H_8 selectivity. The selectivity was further confirmed by performing C_3H_6/C_3H_8 50/50 mixed-gas column break-

through experiments (Fig. 3C), imitating the real conditions for the C_3H_6/C_3H_8 separation process, at room temperature and 1 bar in a packed column bed of ~1.4 g of NbOFFIVE-1-Ni. By using 4 cm³/min total gas flow, C_3H_8 was not adsorbed in the packed column bed, whereas pure C_3H_6 was retained for ~480 s (Fig. 3C). Additionally, mixed-gas column breakthrough experiments were performed in dilute conditions by using N_2 as a carrier inert gas, namely C_3H_6/ C_3H_8/N_2 in 5/5/90 (fig. S25) and $C_3H_6/C_3H_8/N_2$ in 25/25/90 (fig. S26) mixtures. The pure C_3H_6 was retained in the packed column bed, whereas N_2 and C_3H_8 were not adsorbed or retained by NbOFFIVE-1-Ni. The regeneration and activation of the saturated adsorbent, desorption over a 10-min period, showed solely the propylene signal and thus confirmed the nonadsorption and nonretention of the propane in the bed (fig. S27).

To support and confirm the complete molecular exclusion of C_3H_8 and the sole adsorption of C_3H_6, simultaneous calorimetric and gravimetric measurements (thermogravimetry–differential scanning calorimetry) were performed at 1 bar. This confirmed the complete exclusion of propane from propylene, as evidenced by the lack of a detectable heat of adsorption in the case of C_3H_8, as compared with the heat of adsorption for C_3H_6 of 57.4 kJ/mol (Fig. 3D). High-pressure adsorption studies confirmed the nondetectable adsorption of C_3H_8 below 1.5 bar, and only minor propane uptake was observed at ~1.5 bar (~0.1 mol/kg) (fig. S11).

Prior C_3H_6/C_3H_8 adsorption studies—using zeolite, carbon molecular sieves (CMSs), or MOFs—revealed the plausible equilibrium- and/or kinetic-based separation but with low to moderate separation factors (7, 27–29). Correspondingly, the evaluation of zeolite molecular sieves for the propylene/propane separation under similar experimental conditions as the NbOFFIVE-1-Ni adsorbent revealed (i) the very poor C_3H_6/C_3H_8 separation (fig. S12) for zeolite 4A at 1 bar total pressure, as a result of the very slow C_3H_6 adsorption kinetics (fig. S13), and (ii) the extremely low selectivity of nearly 2 for zeolite 5A, despite its associated fast adsorption kinetics relative to that of NbOFFIVE-1-Ni (fig. S13).

The deployment of NbOFFIVE-1-Ni as a splitter agent or adsorbent, permitting the complete sieving of C_3H_8 from C_3H_6, offers (i) a simplified separation process based on a concentration swing recycling mode (CSRM) or a vacuum swing recycling mode (VSRM), in which the ideal working C_3H_6 capacity can be accomplished by performing a desorption step with an inert gas (such as He or N_2) purge at 1.2 bar or by simply reducing the pressure from 1.2 bar to 0.01 bar (Fig. 3B); and (ii) the ability to eliminate the energy-demanding high-pressure steps used in the case of the zeolite 4A adsorbent—pressurization (step 2), purge (with N_2, step 3), and cocurrent blow down (step 4) will not be required in the projected concentration swing adsorption (CSA) or vacuum swing adsorption (VSA) system when using the NbOFFIVE-1-Ni adsorbent (Fig. 4B). The implementation of the VSA system based on NbOFFIVE-1-Ni as an
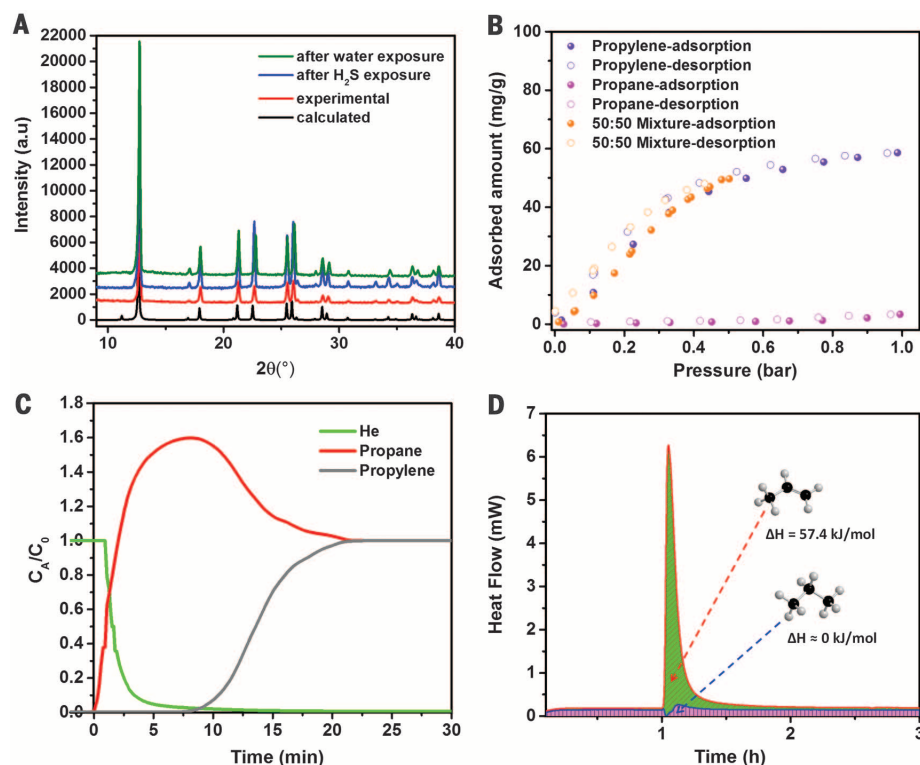

Fig. 3. Evaluation of the chemical stability and propylene/propane separation ability of NbOFFIVE-1-Ni. (A) Powder x-ray diffraction experiments showing the stability of NbOFFIVE-1-Ni after exposure to water and H_2S. **(B)** The pure C_3H_8 (pink), pure C_3H_6 (purple), and equimolar mixture of C_3H_6/C_3H_8 50/50 (orange) isotherms of NbOFFIVE-1-Ni have been collected at 298 K, demonstrating the full propylene from propane sieving ability of this adsorbent at 1 bar. **(C)** C_3H_6/C_3H_8 50/50 mixed-gas experiment using a packed column bed at 298 K and a 1 bar total pressure and 4 cm³/min total flow, confirming the infinite C_3H_6/C_3H_8 separation factor. **(D)** Calorimetric measurements of C_3H_8 and C_3H_6 adsorption on NbOFFIVE-1-Ni were performed so as to quantify the heat of adsorption of propylene and to reaffirm the exclusion/no adsorption of propane.

Fig. 4. Separation process based on concentration swing recycling mode and a simplified CSA or VSA system for the NbOFFIVE-1-Ni molecular sieve. (**A**) C_3H_6/C_3H_8 50/50 mixed-gas 11 cyclic experiments for NbOFFIVE-1-Ni at 298 K and 1 bar, with 4 cm³/min total flow and using a CSRM system, with He as a purge gas for cycles 2 to 10, whereas the sample was activated for 8 hours at 105°C under vacuum for cycle 1 and cycle 11. (**B**) Principle of using NbOFFIVE-1-Ni as a C_3H_8 sieve in two-step CSA or VSA (red line, steps 1 and 5) as compared with a pressure swing adsorption (PSA) system using the zeolite 4A (steps 1 through 5).
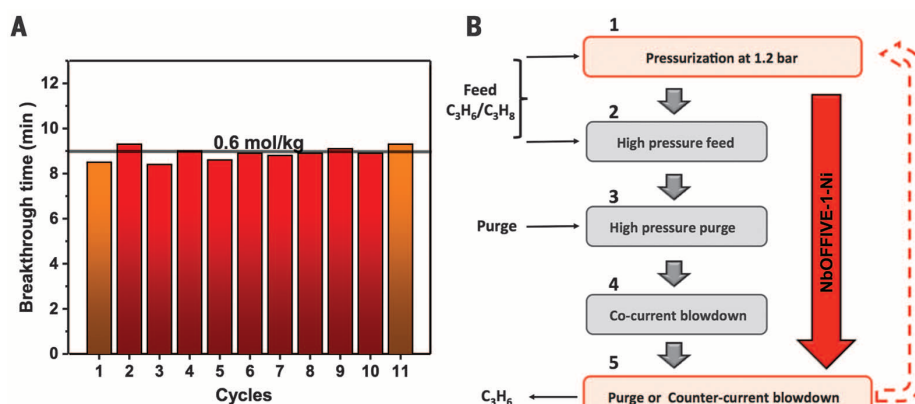
adsorbent offers the potential to considerably reduce the energy penalty associated with the conventional C_3H_6/C_3H_8 separation, and valuably recover both C_3H_6 and C_3H_8 separately in a high-purity grade.

Correspondingly, we performed subsequent mixed-gas (C_3H_6/C_3H_8 at 50/50) column breakthrough measurements in order to corroborate the preservation of the adsorption properties and separation performance of the NbOFFIVE-1-Ni—the propylene adsorption uptake and the full molecular exclusion of propane from propylene at standard ambient temperature and pressure. The multiple adsorption/desorption measurements (over 10 cycles) by use of CSRM revealed that NbOFFIVE-1-Ni maintained its propylene adsorption capacity and its full molecular exclusion of propane (Fig. 3C and figs. S14 to S23). Conversely, the deployment of the aforementioned CSRM protocol under the same operating conditions in the case of the evaluated zeolite molecular sieves revealed a noticeable decrease in the C_3H_6 retention time by the zeolite 5A, which is equivalent to a 300% reduction after only four adsorption/desorption cycles (fig. S24). In the case of zeolite 4A, the low propylene uptake associated with its very slow diffusion limited the scope of zeolite 4A for the C_3H_6/C_3H_8 separation under atmospheric conditions.

Detailed analysis of the data, for the C_3H_6/C_3H_8 50/50 mixed-gas adsorption cycles in a bed composed of 1.4 g of NbOFFIVE-1-Ni, indicated a C_3H_6 uptake of ~0.6 mol/kg for a given cycle based on an 8-min adsorption followed by a 10-min desorption (Fig. 3C) when using CSRM. This result pinpoints the appropriateness of the NbOFFIVE-1-Ni as a stable separating agent for propylene/propane, with a pronounced propylene uptake/recovery of ~2 mol/kg/hour. The NbOFFIVE-1-Ni adsorbent offers potential to effectively separate propylene from propane with a reduced energy footprint by using a CSA. The zeolite 4A, when using VSA at high pressure and 423 K, offers only a limited 26% recovery for a propylene capacity of 1.03 mol/kg/hour (0.13 mol/kg per cycle), with a 97% purity (*30*).

We have demonstrated the successful use of reticular chemistry to deliberately fabricate a fluorinated MOF adsorbent, with controlled pore

aperture size and shape, for the selective molecular exclusion of propane from propylene at standard ambient temperature and pressure, up to 1.5 bar. This complete molecular sieving of propane from propylene was supported by a combined comprehensive study on the basis of single-gas, mixed-gas adsorption and calorimetric-gravimetric experiments. The NbOFFIVE-1-Ni adsorbent possesses a noticeably high chemical stability—as demonstrated by its tolerance to water vapor and hydrogen sulfide—and high thermal stability. The full molecular exclusion of propane by NbOFFIVE-1-Ni adsorbent provides the potential to deploy a simplified and energy-efficient concentration swing adsorption system that does not require energy-demanding steps such as pressurization, high-pressure purge, or cocurrent blow down.

This study illustrates the merit of the molecular building block approach in MOF chemistry for the ultrafine-tuning of the pore aperture size and shape to address important gas separations. Evidently, high porosity is not a sorbent perquisite for an effective and efficient gas separation; a nonporous material to the N_2 adsorbate at cryogenic temperature—a routine probe to assess the microporosity of a given adsorbent such as KAUST-7—can possess distinctive gas separation properties that can be revealed and disclosed through the close examination of the material structural features and the subsequent deeper examination and evaluation of its gas adsorption properties at room temperature.

REFERENCES AND NOTES

1. U.S. Department of Energy (DOE), *Materials for Separation Technology: Energy and Emission Reduction Opportunities* (DOE, 2005).
2. P. Bai *et al.*, *Nat. Commun.* **6**, 5912 (2015).
3. A. Chauvel, G. Lefebvre, in *Petrochemical Processes* (Gulf Publishing, 1989), pp. 199–208.
4. D. J. Safarik, R. B. Eldridge, *Ind. Eng. Chem. Res.* **37**, 2571–2581 (1998).
5. R. T. Yang, E. S. Kikkinides, *AIChE J.* **41**, 509–517 (1995).
6. M. C. Campo *et al.*, *Separ. Purif. Tech.* **103**, 60–70 (2013).
7. J. Liu *et al.*, *Carbon* **85**, 201–211 (2015).
8. C. A. Grande, J. Gascon, F. Kapteijn, A. E. Rodrigues, *Chem. Eng. J.* **160**, 207–214 (2010).
9. C. A. Grande, A. E. Rodrigues, *Ind. Eng. Chem. Res.* **44**, 8815–8829 (2005).
10. A. H. Assen *et al.*, *Angew. Chem. Int. Ed. Engl.* **54**, 14353–14358 (2015).
11. G. Férey, *Chem. Soc. Rev.* **37**, 191–214 (2008).
12. S. Kitagawa, R. Kitaura, S. Noro, *Angew. Chem. Int. Ed. Engl.* **43**, 2334–2375 (2004).
13. M. Eddaoudi *et al.*, *Acc. Chem. Res.* **34**, 319–330 (2001).
14. A. R. Millward, O. M. Yaghi, *J. Am. Chem. Soc.* **127**, 17998–17999 (2005).
15. D. Fairen-Jimenez *et al.*, *Chem. Commun.* **48**, 10496–10498 (2012).
16. Y. Peng *et al.*, *J. Am. Chem. Soc.* **135**, 11887–11894 (2013).
17. Q. Yang *et al.*, *Chem. Commun.* **48**, 9831–9833 (2012).
18. D.-X. Xue *et al.*, *J. Am. Chem. Soc.* **137**, 5034–5040 (2015).
19. P. Nugent *et al.*, *Nature* **495**, 80–84 (2013).
20. K. Sumida *et al.*, *Chem. Rev.* **112**, 724–781 (2012).
21. S. Xiang *et al.*, *Nat. Commun.* **3**, 954 (2012).
22. Z. R. Herm, R. Krishna, J. R. Long, *Micropor. Mesopor. Mater.* **151**, 481–487 (2012).
23. O. M. Yaghi *et al.*, *Nature* **423**, 705–714 (2003).
24. O. Shekhah *et al.*, *Nat. Commun.* **5**, 4228 (2014).
25. H. K. Izumi, J. E. Kirsch, C. L. Stern, K. R. Poeppelmeier, *Inorg. Chem.* **44**, 884–895 (2005).
26. R. Gautier, M. D. Donakowski, K. R. Poeppelmeier, *J. Solid State Chem.* **195**, 132–139 (2012).
27. O. Shekhah *et al.*, *Chem. Commun.* **50**, 2089–2092 (2014).
28. E. D. Bloch *et al.*, *Science* **335**, 1606–1610 (2012).
29. X. Yang, B. H. Toby, M. A. Camblor, Y. Lee, D. H. Olson, *J. Phys. Chem. B* **109**, 7894–7899 (2005).
30. F. A. Da Silva, A. E. Rodrigues, *Ind. Eng. Chem. Res.* **40**, 5758–5774 (2001).

Editor's Summary

Separating one organic from another

Separating closely related organic molecules is a challenge (see the Perspective by Lin).The separation of acetylene from ethylene is needed in high-purity polymer production. Cui et al. developed a copper-based metal-organic framework with hexafluorosilicate and organic linkers designed to have a high affinity for acetylene. These materials, which capture four acetylene molecules in each pore, successfully separated acetylene from mixtures with ethylene. Propane and propylene are both important feedstock chemicals. Their physical and chemical similarity, however, requires energy-intense processes to separate them. Cadiau et al. designed a fluorinated porous metal-organic framework material that selectively adsorbed propylene, with the complete exclusion of propane.

Article Tools	Visit the online version of this article to access the personalization and article tools: http://science.sciencemag.org/content/353/6295/137
Permissions	Obtain information about reproducing this article: http://www.sciencemag.org/about/permissions.dtl